Learning Spatio-Temporal Features with Two-Stream Deep 3D CNNs for Lipreading

Xinshuo Weng
http://www.xinshuoweng.com

Kris Kitani
http://www.cs.cmu.edu/~kkitani

Robotics Institute
School of Computer Science
Carnegie Mellon University
Pittsburgh, USA

Abstract

We focus on the word-level visual lipreading, which requires recognizing the word being spoken, given only the video but not the audio. State-of-the-art methods explore the use of end-to-end neural networks, including a shallow (up to three layers) 3D convolutional neural network (CNN) + a deep 2D CNN (*e.g.*, ResNet) as the front-end to extract visual features, and a recurrent neural network (*e.g.*, bidirectional LSTM) as the back-end for classification. In this work, we propose to replace the shallow 3D CNNs + deep 2D CNNs front-end with recent successful deep 3D CNNs — two-stream (*i.e.*, grayscale video and optical flow streams) I3D. We evaluate different combinations of front-end and back-end modules with the grayscale video and optical flow inputs on the LRW dataset. The experiments show that, compared to the shallow 3D CNNs + deep 2D CNNs front-end, the deep 3D CNNs front-end with pre-training on the large-scale image and video datasets (*e.g.*, ImageNet and Kinetics) can improve the classification accuracy. Also, we demonstrate that using the optical flow input alone can achieve comparable performance as using the grayscale video as input. Moreover, the two-stream network using both the grayscale video and optical flow inputs can further improve the performance. Overall, our two-stream I3D front-end with a Bi-LSTM back-end results in an absolute improvement of 5.3% over the previous art on the LRW dataset.

1 Introduction

Word-level visual lipreading, the ability to recognize the word being spoken from visual information alone, is a challenging task for both human and machine due to its ambiguity. As the McGurk effect introduced in [24], different characters can produce similar lip movement (*e.g.*, 'p' and 'b'). These characters, called homophones, are difficult to be determined from visual cues alone. However, people have demonstrated that this ambiguity can be resolved to some extent using the context of neighboring characters in a word (*i.e.*, word-level lipreading). Therefore, modeling the temporal context between frames is very important to recognize the nearby characters. In this work, we apply recent successful deep 3D convolutional neural networks (CNNs) to learn the temporal context for word-level visual lipreading.

Traditionally, researchers have approached the visual lipreading by a two-stage pipeline, including feature extraction from the mouth region and classification using the sequence model, in which the process in two stages are independent. The most common feature extraction approaches use a dimension reduction or compression method, with the most popular
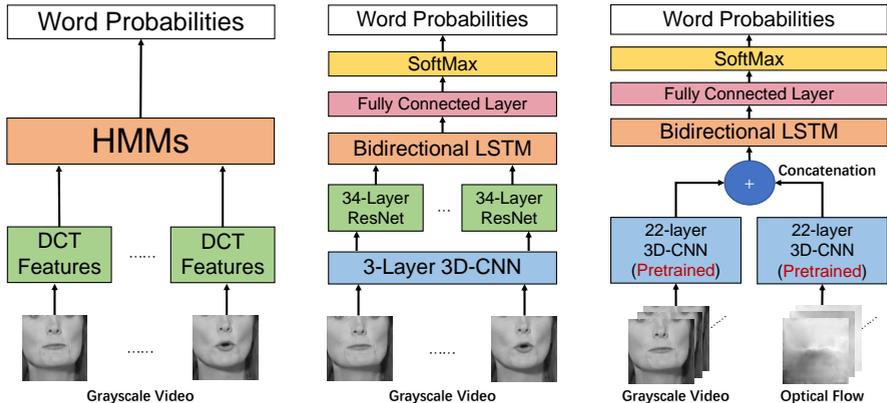
Figure 1: **Comparison of the Lipreading Pipeline**: traditional two-stage pipeline (**left**), end-to-end neural network based pipeline (**middle**) and the proposed pipeline (**right**). The proposed one is the first investigating deep 3D CNNs beyond three layers for lipreading.

being the Discrete Cosine Transform (DCT) [28, 32, 33, 49]. This yields us compact image-based features of the mouth. In the second stage, a sequence model, such as the Hidden Markov Model (HMM) [10, 36, 39], is used to model the temporal dependency from the extracted features for classification.

Recently, deep learning approaches for visual lipreading [2, 19, 26, 27, 30, 31, 40, 43, 45, 47] have been proposed and achieved the state-of-the-art performance, in which the two-stage pipeline is replaced with the end-to-end trainable neural networks. Similar to the traditional methods, a sequence of the cropped mouth is fed into a front-end to extract the visual features, which are then passed to a back-end to model the temporal dependency for classification. As the gradients computed from the loss can flow back from the back-end module to the front-end module, the entire network is end-to-end trainable such that the learned features are more suitable for lipreading than the standalone features used in the traditional methods. Specifically, existing works usually use the combination of a shallow 3D CNN (up to three 3D layers) and a deep 2D CNN (*e.g.*, ResNet [14]) as the front-end, and use the bi-directional recurrent neural network (*e.g.*, Bi-LSTM) as the back-end.

However, it is commonly accepted that image-based features extracted from the 2D CNNs are not directly suitable for video task (*e.g.*, visual lipreading). Intuitively, it is more natural to use the 3D CNNs as the front-end to learn spatial-temporal features. Surprisingly, only a few works [1, 3, 31, 45], to the best of our knowledge, have explored the use of 3D CNNs for lipreading. Also, only a shallow 3D CNN (up to three 3D convolutional layers) is used in those works, in which the network architecture design is contradictory to our common knowledge that a deep neural network is expected to do better than a shallow one. We conclude that the deep 3D CNNs with a large number of parameters will easily over-fit on lipreading datasets and perform even worse than the model with the shallow 3D CNNs + deep 2D CNNs front-end, which does not have a severe over-fitting problem when training on standard lipreading datasets. In addition, we observe that no prior work has explored the use of optical flow for visual lipreading, although the optical flow has been proved to be very useful in many video tasks [4, 17, 37].

In this paper, we present the first word-level lipreading pipeline *with the use of deep 3D CNNs and optical flow*. We compared the proposed pipeline with traditional and recent deep

learning based pipelines in Figure 1. To the best of our knowledge, this is the first work investigating the deep 3D CNNs beyond three layers and optical flow input for lipreading. For deep 3D CNNs, we use a 3D version of 22-layer Inception network (I3D [5]), first proposed for video action recognition, as our front-end. To handle the over-fitting problem caused by the increased number of parameters from the 3D kernels, we borrow the idea from [5] to inflate the pre-trained weights of the 2D Inception network on the ImageNet [21] into three dimensions as the initialization of the 3D kernels. Moreover, with the conclusion from [12] that a 3D CNN can be fine-tuned to achieve better performance on other video datasets when first pre-trained on large-scale video datasets, we thus perform a second-round pre-training on the Kinetics [5] dataset, which is a large-scale video dataset.

We evaluate different combinations of front-end and back-end modules on the challenging LRW dataset. The experiments show that, compared to the shallow 3D CNNs + deep 2D CNNs front-end, the deep 3D CNNs front-end with pre-training on the large-scale image and video datasets (*e.g.*, ImageNet and Kinetics) can improve the classification accuracy for visual lipreading. Also, to show the effectiveness of the optical flow input in lipreading, we replace the conventional grayscale video input with pre-computed optical flow. The conclusion is that using the optical flow input alone can achieve comparable performance as using the grayscale video as input. Furthermore, a two-stream network using both the grayscale and optical flow inputs can further improve the performance. Overall, our two-stream I3D front-end with a Bi-LSTM back-end results in an absolute improvement of 5.3% over previous state-of-the-art methods on the LRW dataset.

Our contributions are summarized as follows: (1) we present the first work which applies the deep 3D CNNs beyond three layers for word-level visual lipreading; (2) we demonstrate that pre-training on the large-scale image and video dataset is important when training the deep 3D CNNs for lipreading; (3) we show empirically that using the optical flow as an additional input to the grayscale video in a two-stream network can further improve the performance; (4) our proposed two-stream I3D front-end with a Bi-LSTM back-end achieves the state-of-the-art performance on standard lipreading benchmark.

2 Related Work

Word-Level Visual Lipreading. Existing methods to approach word-level lipreading by using visual information alone can be mostly split into two categories. The first category method, shown in the Figure 1 (left), is mainly composed of two separate stages involving the feature extraction from the mouth region and classification using the sequence model, in which the process in two stages are independent. Variants in this category are different in having a different data pre-processing procedure or using different feature extractors and classifiers. [28] proposes a DCT coefficient selection procedure, which prefers the higher-order vertical components of the DCT coefficients, to achieve better performance when the variety of the hand pose is large in the dataset. [32] proposes a new cascaded feature extraction process including not only the DCT features but also a linear discriminant data projection and a maximum likelihood-based data rotation. [49] proposes a PCA-based method to reduce the dimension of the DCT-based features.

Although this category methods with the two-stage pipeline have made significant progress over the decades, all methods in this category separate the feature extraction process from the classifier's training process, causing that the extracted features might not be the best suitable for word classification.

The second category methods, shown in Figure 1 (middle), approach the visual lipreading

based on the recent advance of deep learning. The major difference from the first category methods is that the two-stage process no longer exists. Instead, the entire system composed of a front-end and back-end neural network is end-to-end trainable, and thus the learned features are more related to the specific task that the network is trained on. [27] is the first work which proposes to use the CNNs as the front-end to replace the independent feature extractor used in the traditional methods. [2] proposes a speaker-adaptive training procedure to achieve a speaker-independent lipreading system with the use of deep neural networks. [47] is the first proposing to use the LSTM [15] as the back-end for classification and has shown a significant improvement over the traditional classifiers. [19] takes advantage of the proposed large-scale lipreading dataset and train a VGG-like front-end for lipreading. Beyond [19], [6] also shows the effectiveness of adding the LSTM module at the end for word classification. Furthermore, [3, 45] propose to use a shallow 3D CNN (up to three 3D convolutional layers) in combination with a strong deep 2D CNN — ResNet — as the front-end in the lipreading system. Similarly, [4] uses three 3D convolutional layers for sentence-level lipreading. Beyond using visual features, [31] proposes a neural network to extract the audio features and fuses with the visual features.

Surprisingly, we find that the existing methods in this category have only explored to use the deep 2D CNNs, shallow 3D CNNs or their combination for video feature extraction in lipreading. In contrast, our proposed method is the first work investigating the benefit of using a deep 3D CNN as the front-end for visual lipreading and has demonstrated a significant improvement over previous state-of-the-art methods.

Neural Network Architectures for Video Feature Extraction. Researchers have developed CNN architectures specifically for video understanding for a long time. To re-use the ImageNet [21] pre-trained weights, [20] proposes to extract features independently from each frame using a 2D CNN and then pool the features to predict the action. More satisfying approaches [9, 25] add a recurrent neural network as the back-end, such as a LSTM, instead of a pooling layer to capture the temporal dependency and compensate the disadvantages of the 2D CNNs. In addition, as the optical flow can encode the motion information directly, [1, 37, 43, 50] propose the two-stream networks, which has an additional optical flow stream to extract the motion features using the 2D CNNs. On the other hand, a natural extension of the 2D convolution for video data is the 3D convolution. [18, 44, 46] propose to use the 3D CNNs for video action recognition. Beyond using the shallow 3D CNNs, 3D-ResNet [13, 22] explores the 3D version of the deep 2D CNNs — ResNet — by replacing all 2D operations with their 3D counterparts, outperforming the 2D CNNs+LSTM and two-stream 2D CNNs paradigms. To alleviate the over-fitting problem when training the deep 3D CNNs, P3D-ResNet [34] proposes to decompose the 3D convolution with a 2D convolution along the spatial dimension and 1D convolution along the temporal dimension. As a natural combination of the two-stream networks and deep 3D CNNs, [5] proposes a two-stream deep 3D CNN (I3D) pre-trained on the large-scale video dataset — Kinetics, achieving the state-of-the-art performance on action recognition. Furthermore, [23] employs the same I3D network for collision prediction. In this paper, we apply a similar idea (*i.e.*, the two-stream deep 3D CNNs) and aim at transferring the success to visual lipreading.

3   Lipreading Framework

In Figure 2, we decompose the lipreading framework into four parts: (a) inputs, which can be a sequence of grayscale images, optical flow data, or the combination of them; (b) a front-end module, to extract the features from the inputs; (c) a back-end module, to model
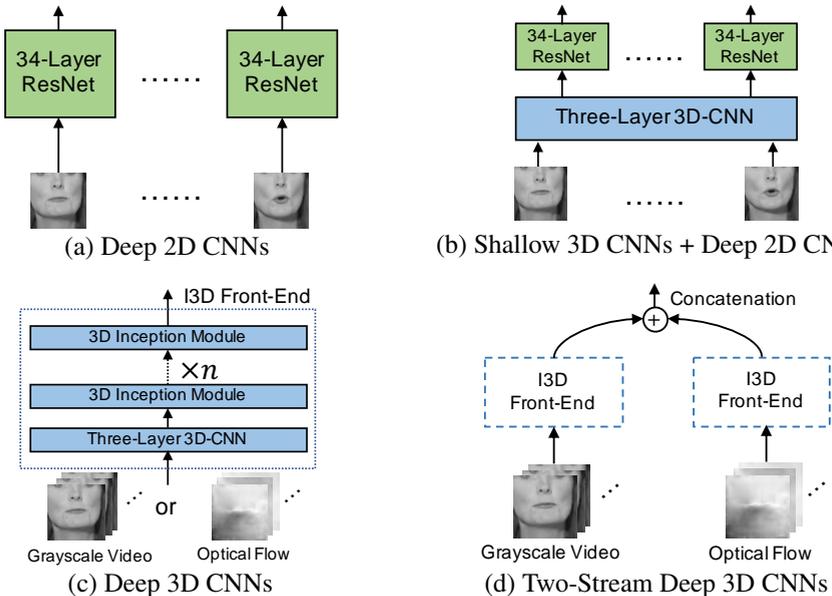
(a) Deep 2D CNNs

(b) Shallow 3D CNNs + Deep 2D CNNs

(c) Deep 3D CNNs

(d) Two-Stream Deep 3D CNNs

Figure 3: **Comparison of the Front-End Modules**: (a) a deep 2D ResNet is used to extract features independently for each frame; (b) a shallow (three-layer) 3D CNN is added before the ResNet; (c) a deep (22-layer) I3D (Inflated 3D ConvNets) front-end learns the spatial-temporal features from either the grayscale video or the optical flow data; (d) a two-stream I3D concatenates the features extracted from both the grayscale video and optical flow data.

the temporal dependency and summarize the features into a single vector which represents the raw score for each word; (d) a softmax layer, to compute the probabilities of each word. With above definition of the lipreading framework, we claim that most of the existing lipreading methods, and the proposed method, fall into it. In this paper, we focus on the inputs and front-end modules which will be introduced in the following sections. We will show how different combinations of them will affect the lipreading performance.
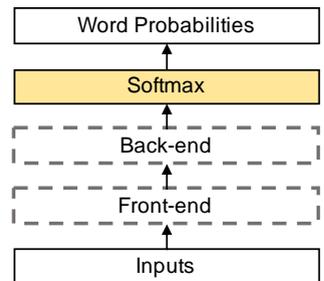

Figure 2: Lipreading framework

3.1 Front-End Modules

We compare the deep learning based front-end modules for visual lipreading progressively in terms of the complexity of the network. Figure 3 shows the front-end modules that will be discussed in this paper.

3.1.1 Recap: Deep 2D CNNs

The 2D CNNs are originally proposed to solve image-based tasks [14, 21, 58, 42]. When working with the video data in visual lipreading, we can concatenate the features extracted independently from each frame. Although the features extracted from the deep 2D CNNs front-end only contain the image-based information, the following back-end module such as a recurrent neural network can model the temporal dependency to some extent. We con-

sider the deep 2D CNNs as one of our baseline front-end modules, shown in Figure 3 (a). Specifically, we use the 34-layer ResNet to extract the features from the grayscale video.

3.1.2 Recap: Shallow 3D CNNs + Deep 2D CNNs

In addition to using the deep 2D CNNs, existing works [3, 45] investigate using a shallow 3D CNN to pre-process the grayscale video before applying the deep 2D CNNs. It is commonly known that the 3D convolution can capture the short-term dynamics and is proven to be advantageous in visual lipreading even when the recurrent networks are deployed for the back-end. However, due to the difficulty of training a huge number of parameters introduced by the three-dimensional kernels, state-of-the-art methods in lipreading have only explored the shallow 3D CNNs with no more than three layers. We consider this shallow 3D CNNs + deep 2D CNNs as another strong baseline front-end module, shown in Figure 3 (b). Specifically, we pass the grayscale video through three 3D convolutional layers with 64, 64 and 96 kernels of a size of $3\times5\times5$, $3\times5\times5$ and $3\times3\times3$ (time/width/height) respectively, each followed by the batch normalization [16], Rectified Linear Units (ReLU)[1] and 3D max-pooling layer with a size of $1\times2\times2$. The extracted features are then processed by the 34-layer ResNet on each channel of features.

3.1.3 Deep 3D CNNs

Although the shallow 3D CNNs are proven to be helpful, the effect of only using three-layer 3D convolutional layers might not hit the maximum. Also, the temporal dynamics encoded in the features extracted from the shallow 3D CNNs might be impaired by the following 2D CNNs. Therefore, it is natural to use the deep 3D CNNs alone to replace the shallow 3D CNNs + deep 2D CNNs front-end. Specifically, we consider the successful Inflated 3D ConvNets (I3D [5]), the state-of-the-art 3D CNNs and first proposed for video action recognition, as our deep 3D CNNs front-end, shown in Figure 3 (c). The I3D front-end contains

Figure 4: 3D inception module.

twenty-two 3D convolutional layers including three 3D convolutional layers with 64, 96 and 192 kernels of a size of $7\times7\times7$, $3\times3\times3$ and $3\times3\times3$ respectively, 3D max-pooling layer with a size of $1\times2\times2$, and a series of 3D inception modules (the 3D extension of the 2D inception [42] module), shown in Figure 4.

3.1.4 Two-Stream Deep 3D CNNs

In theory, deep 3D CNNs are expected to extract strong enough spatial-temporal features from the gray-scale video inputs. In practice, fusing an additional optical flow stream with the grayscale video
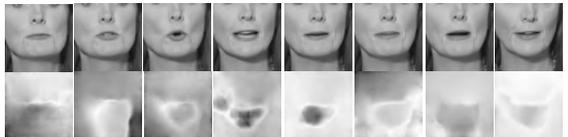

Figure 5: Examples of images and corresponding flow.

stream is proven to be useful in many video tasks [4, 17, 37], as the optical flow can explicitly capture the motion of pixels in adjacent images, represented by the direction and magnitude of the motion of each pixel. Specifically, we use the PWC-Net [41] to
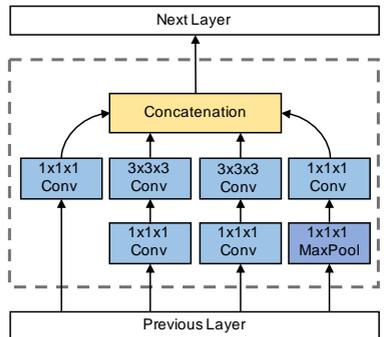
---

[1]Each 3D convolutional layer will be followed by the batch normalization and ReLU by default, and will not be mentioned again in the following sections.

pre-compute the optical flow. Examples are shown in Figure 5. We then use another I3D front-end (employing the same architecture as the I3D front-end in grayscale video stream but not sharing weights) to extract the features from the optical flow and concatenate with the features extracted from the grayscale video stream. We illustrate our two-stream deep 3D CNNs in Figure 3 (d).

3.2 Back-End Modules

3.2.1 1D Temporal ConvNets (TC)

In the simplest setting, we can just use the 1D convolution operating along the temporal channel to aggregate the information for word prediction. We consider this 1D temporal ConvNets as our baseline back-end, shown in Figure 6. Specifically, we use two 1D convolutional layers operating along the temporal dimension followed by a fully connected layer which maps the length of the vector to the number of words in order to compute the raw score for each word. In detail, the first 1D convolutional layer has 512

Figure 6: 1D Temporal ConvNets back-end.

kernels with a kernel size of 5 and a stride of 2, followed by a max-pooling layer with a kernel size of 2 and a stride of 2. The second 1D convolutional layer has 1024 kernels with the same kernel size and stride as the first one.
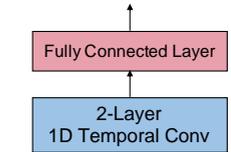
3.2.2 Bidirectional LSTM

Recurrent neural networks (RNNs) are well known to model temporal dependency and are typical back-end modules used in visual lipreading. Among RNNs, LSTM is proven to be useful when dealing with the exploding and vanishing gradient problems. On the other hand, bidirectional RNNs [35] are the widely used technique allowing RNNs to have both backward and forward information about the sequence at every time step. Combining both, we use the bidirectional LSTM (Bi-LSTM) as our back-end module, shown in Figure 7. Specifically, we use a two-layer bidirectional LSTM with a hidden state dimension of 256 for each cell. At the last layer of Bi-LSTM, we concatenate the features from two directions and average

Figure 7: Two-layer bidirectional LSTM back-end.

the features along the temporal dimension, resulting in the features with a dimension of 512. We then pass the features through a linear layer with a dimension of 512×500, in order to map to the raw score for each word.
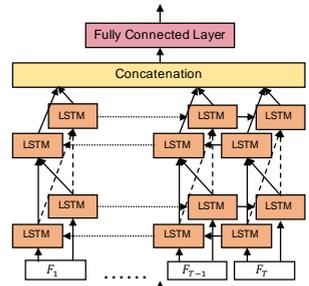
4 Two-Round Pre-Training

ImageNet pre-trained weights are proven to be useful in many image-based tasks. However, it is not possible to directly use the ImageNet pre-trained weights as the initialization of the 3D kernels because the 3D kernels have an additional dimension of weights. Following [6], we inflate the ImageNet pre-trained weights into three dimensions by repeating the weights of the 2D filters N times along the temporal dimension and use inflated weights as the initialization of our I3D front-end. However, such inflated weights pre-trained on the ImageNet can only extract spatial features independently for each channel. With the conclusion from [12], when pre-trained on the large-scale video datasets, a deep 3D CNN can eventually achieve better performance on other video datasets after fine-tuning. Therefore, we have

a second-round pre-training on the large-scale video dataset — Kinetics [5], such that the pre-trained 3D kernels can be directly suitable for extracting the spatial-temporal features.

5 Dataset

We train and evaluate the proposed networks on the word-level lipreading dataset LRW [19]. The dataset contains short clips of videos (488,766 for training, 25,000 for validation and 25,000 for testing) extracted from the BBC TV broadcasts (*e.g.*, News and Talk Shows). There are 29 frames of grayscale images for each video sequence. LRW dataset is characterized by its high variability regarding speakers and pose. The number of target words is 500, which is an order of magnitude higher than other publicly available databases (*e.g.*, GRID [8] and CUAVE [29]). The other feature is the existence of pairs of words that share most of their visemes. Such examples are nouns in both singular and plural forms (e.g. benefit-benefits, 23 pairs) as well as verbs in both present and past tenses (e.g. allow-allowed, 4 pairs). Perhaps the most difficult part of the dataset is the fact that the target words appear within utterances rather than being isolated. Hence, the network should learn not merely how to discriminate between 500 target words, but also how to ignore the irrelevant parts of the utterance and spot one of the target words. Also, the network should learn how to do so without knowing the word boundaries.

6 Data Pre-Processing and Augmentation

Cropping the Mouth Region. As the video provided by the LRW dataset contains the entire faces of the speakers and the surrounding background, which are the irrelevant contexts for identifying the spoken words, we crop the original video using a fixed bounding box with the size of 112×112 centered at the mouth region, convert the RGB images to grayscale images and normalize them with respect to the overall mean and variance of the dataset. Some random sequences of the cropped mouth from the LRW dataset before the normalization are shown in Figure 8.

Figure 8: Cropped mouth region and the corresponding labels from the LRW dataset.

Data Augmentation. We follow the conventional data augmentation mechanisms for visual lipreading during training, including random horizontal flip and cropping (±5 pixels) so that the training images are not perfectly centered at the mouth which might be the case during the testing. When using the two-stream networks, we augment the data in the same way for both two streams so that the data in two streams are well aligned spatially.

7 Experiments

7.1 Comparison with State-of-the-Art

We summarize the top-1 word accuracy of the state-of-the-art word-level lipreading methods and our proposed one on the LRW dataset in Table 1. Our final model, which is composed of a two-stream (grayscale video and flow streams) deep 3D CNNs front-end with two-round pre-training and a bidirectional LSTM back-end, outperforms all previous state-of-the-art methods whose front-ends are the deep 2D CNNs or

Table 1: Quantitative comparison of top-1 accuracy on the LRW dataset.

Method	Val / %	Test / %
[19]	-	61.10
[5]	-	66.00
[7]	-	76.20
[45]	78.95	78.77
Ours	**84.11**	**84.07**

Table 2: Ablative analysis of top-1 accuracy on the LRW dataset.

Index	Inputs		Front-End			Back-End		Pre-Training	Val / %	Test / %
	grayscale	flow	shallow 3D	deep 2D	I3D	1D TC	Bi-LSTM			
(a)	✓		✓	✓		✓			71.19	70.85
(b) [15]	✓		✓	✓			✓		78.95	78.77
(c)	✓			✓			✓		75.37	75.23
(d)	✓			✓			✓	ImageNet	75.69	74.98
(e)	✓				✓		✓		59.11	59.45
(f)	✓				✓		✓	Two-Round	81.73	81.52
(g)		✓	✓	✓			✓		77.65	77.23
(h)		✓			✓		✓	Two-Round	82.17	82.93
(i)	✓	✓	✓	✓			✓		80.11	80.34
(j) **Ours**	✓	✓			✓		✓	Two-Round	**84.11**	**84.07**

shallow 3D CNNs with only grayscale video input. On the LRW dataset, our method establishes new state-of-the-art performance and improves the accuracy from 78.77 of prior art [15][2] to 84.07 on the test set.

7.2 Ablation Study

We conduct the ablative analysis by evaluating the performance of the lipreading networks with different combinations of front-end and back-end modules introduced in previous sections. We use the top-1 word classification accuracy as our evaluation metric on both the validation and testing sets.

Evaluating the Back-End Modules. We first focus on the back-end modules by comparing the Bi-LSTM with the 1D temporal ConvNets while fixing the inputs as the grayscale video and the front-end module as the shallow 3D CNNs + Deep 2D CNNs. The results are shown in Table 2 (a) and (b). Clearly, using Bi-LSTM as the back-end module is better than using 1D temporal ConvNets. Therefore, we eliminate the 1D temporal ConvNets and only consider the Bi-LSTM as our back-end module in the following experiments.

Evaluating the Effectiveness of Shallow 3D CNNs. As the existing works [3, 15] usually apply a shallow 3D CNN before the deep 2D CNNs in the front-end, we conduct an ablation analysis by removing the shallow 3D CNNs in order to show how important the shallow 3D CNNs are in the front-end. The results are shown in Table 2 (b) and (c). Indeed, adding a few 3D convolutional layers in the front-end can have an obvious accuracy improvement from 75.23% to 78.77% on the test set. Also, to make sure the deep 2D CNNs front-end in (c) is well-performed, we run another ablation analysis shown in Table 2 (d) [3] by using the ImageNet pre-trained weights to initialize the deep 2D CNNs. We find that the results of (c) and (d) are fairly comparable, meaning that the LRW dataset is large enough to train a 34-layer ResNet from scratch without the need for pre-training.

Evaluating the Deep 3D CNNs Front-End and Two-Round Pre-Training. As the major contribution of this paper, here we show the advantages of the deep 3D CNNs front-end over the shallow 3D CNNs + deep 2D CNNs front-end. The results are shown in Table 2 (b) and (f). We show that when the shallow 3D CNNs + deep 2D CNNs front-end in (b) is replaced with the pre-trained I3D front-end in (f), the performance is improved from 78.77%

---

[2]We cannot reproduce the accuracy reported in [15], which is 83.0 on the test set. One possibility is that we do not perform the three-step training as in [15] because we want to make a fair comparison with other methods which are trained end-to-end in one step.

[3]Here we only do the ablation study on using the ImageNet pre-trained weights to initialize the deep 2D CNNs in (c) but not in (b) because it is commonly accepted that using the pre-trained weights to initialize the intermediate layers usually does not help when there are random initialized lower-level layers (*i.e.*, the shallow 3D CNNs in (b)).

to 81.52% on the test set, meaning that the deep 3D CNNs front-end with the two-round pre-training is more powerful than the shallow 3D CNNs + deep 2D CNNs front-end used in previous state-of-the-art methods on the LRW dataset. On the other hand, network in Table 2 (e) using the I3D front-end without pre-training (*i.e.*, training from scratch on the LRW dataset) performs even worse than the previous art shown in (b), which shows that training a deep 3D CNN is much harder and can easily over-fit the LRW dataset, and thus the two-round pre-training is important. In the following experiments, we will use the two-round pre-trained weights to initialize the I3D front-end by default.

Evaluating the Optical Flow Input and Two-Stream Network. To demonstrate if the optical flow input is effective, we replace the grayscale input in (b) and (f) with the pre-computed optical flow. The results are shown in Table 2 (g) and (h). We found that both (g) to (b) and (h) to (f) have comparable performance, meaning that either the optical flow or the grayscale video alone can predict the spoken word. More importantly, we show how the two-stream configuration helps in Table 2 (i) and (j). When comparing the two-stream network with its single-stream counterpart (*i.e.*, either the grayscale stream or the optical flow stream), the performance is clearly improved no matter the front-end is the shallow 3D CNNs + deep 2D CNNs or the pre-trained I3D. This confirms that the two-stream network is beneficial for lipreading. Overall, our two-stream pre-trained I3D + Bi-LSTM (j) achieves an absolute improvement of 5.3% over the previous art in (b).

8   Conclusion

We present the first word-level lipreading pipeline using the deep 3D CNNs (beyond three layers) and optical flow. We evaluate different combinations of front-end and back-end modules on the LRW dataset. We show that, with the two-round pre-training, deep 3D CNNs front-end can outperform the shallow 3D CNNs + deep 2D CNNs front-end used in previous works. On the other hand, we found either the optical flow or grayscale video is effective to be used as input. Moreover, the two-stream network using both optical flow and grayscale video as inputs can further improve the performance. Overall, our proposed word-level lipreading method, which is composed of a two-stream (grayscale video and optical flow streams) pre-trained I3D front-end and a Bidirectional-LSTM back-end, achieves an absolute improvement of 5.3% over the previous art on the LRW dataset.

References

[1] Triantafyllos Afouras, Joon Son Chung, Andrew Senior, Oriol Vinyals, and Andrew Zisserman. Deep Audio-Visual Speech Recognition. *arXiv:1809.02108*, 2018.

[2] Ibrahim Almajai, Stephen Cox, Richard Harvey, and Yuxuan Lan. Improved Speaker Independent Lip Reading Using Speaker Adaptive Training and Deep Neural Networks. *ICASSP*, 2016.

[3] Yannis M Assael, Brendan Shillingford, Shimon Whiteson, and Nando De Freitas. LipNet: End-to-End Sentence-Level Lipreading. *arXiv:1611.01599*, 2017.

[4] Nicolas Bonneel, James Tompkin, Kalyan Sunkavalli, Deqing Sun, Sylvain Paris, and Hanspeter Pfister. Blind Video Temporal Consistency. *ACM SIGGRAPH*, 2015.

[5] Joao Carreira and Andrew Zisserman. Quo Vadis, Action Recognition? A New Model and the Kinetics Dataset. *CVPR*, 2017.

[6] Joon Son Chung and Andrew Zisserman. Learning to Lip Read Words by Watching Videos. *Computer Vision and Image Understanding*, 2018.

[7] Joon Son Chung, Andrew W Senior, Oriol Vinyals, and Andrew Zisserman. Lip Reading Sentences in the Wild. *CVPR*, 2017.

[8] Andrzej Czyzewski, Bozena Kostek, Piotr Bratoszewski, Jozef Kotus, and Marcin Szykulski. An Audio-Visual Corpus for Multimodal Automatic Speech Recognition. *Journal of Intelligent Information Systems*, 2017.

[9] Jeff Donahue, Lisa Anne Hendricks, Marcus Rohrbach, Subhashini Venugopalan, Sergio Guadarrama, Kate Saenko, and Trevor Darrell. Long-Term Recurrent Convolutional Networks for Visual Recognition and Description. *CVPR*, 2015.

[10] Virginia Estellers, Mihai Gurban, and Jean-Philippe Thiran. On Dynamic Stream Weighting for Audio-Visual Speech Recognition. *IEEE Transactions on Audio, Speech, and Language Processing*, 2012.

[11] Christoph Feichtenhofer, Axel Pinz, and Andrew Zisserman. Convolutional Two-Stream Network Fusion for Video Action Recognition. *CVPR*, 2016.

[12] Kensho Hara, Hirokatsu Kataoka, and Yutaka Satoh. Can Spatiotemporal 3D CNNs Retrace the History of 2D CNNs and ImageNet? *CVPR*, 2017.

[13] Kensho Hara, Hirokatsu Kataoka, and Yutaka Satoh. Learning Spatio-Temporal Features with 3D Residual Networks for Action Recognition. *ICCVW*, 2017.

[14] Kaiming He, Xiangyu Zhang, Shaoqing Ren, and Jian Sun. Deep Residual Learning for Image Recognition. *CVPR*, 2016.

[15] Sepp Hochreiter and Jurgen Schmidhuber. Long Short-Term Memory. *Neural Computation*, 1997.

[16] Sergey Ioffe and Christian Szegedy. Batch Normalization: Accelerating Deep Network Training by Reducing Internal Covariate Shift. *ICML*, 2015.

[17] Joel Janai, Fatma Güney, Aseem Behl, and Andreas Geiger. Computer Vision for Autonomous Vehicles: Problems, Datasets and State-of-the-Art. *arXiv:1704.05519*, 2017.

[18] Shuiwang Ji, Ming Yang, and Kai Yu. 3D Convolutional Neural Networks for Human Action Recognition. *TPAMI*, 2013.

[19] Andrew Zisserman Joon Son Chung. Lip Reading in the Wild. *ECCV*, 2016.

[20] Andrej Karpathy, George Toderici, Sanketh Shetty, Thomas Leung, Rahul Sukthankar, and Fei Fei Li. Large-Scale Video Classification with Convolutional Neural Networks. *CVPR*, 2014.

[21] Alex Krizhevsky, Ilya Sutskever, and Geoffrey E Hinton. Imagenet Classification with Deep Convolutional Neural Networks. *NIPS*, 2012.

[22] Kun Liu, Wu Liu, Chuang Gan, Mingkui Tan, and Huadong Ma. T-C3D: Temporal Convolutional 3D Network for Real-time Action Recognition. *AAAI*, 2018.

[23] Aashi Manglik, Xinshuo Weng, Eshed Ohn-bar, and Kris M Kitani. Future Near-Collision Prediction from Monocular Video: Feasibility, Dataset, and Challenges. *arXiv:1903.09102*, 2019.

[24] H. McGurk and J. MacDonald. Hearing Lips and Seeing Voices. *Nature*, 1976.

[25] Joe Yue Hei Ng, Matthew Hausknecht, Sudheendra Vijayanarasimhan, Oriol Vinyals, Rajat Monga, and George Toderici. Beyond Short Snippets: Deep Networks for Video Classification. *CVPR*, 2015.

[26] Hiroshi Ninomiya, Norihide Kitaoka, Satoshi Tamura, Yurie Iribe, and Kazuya Takeda. Integration of Deep Bottleneck Features for Audio-Visual Speech Recognition. *INTERSPEECH*, 2015.

[27] Kuniaki Noda, Yuki Yamaguchi, Kazuhiro Nakadai, Hiroshi G Okuno, and Tetsuya Ogata. Lipreading Using Convolutional Neural Network. *INTERSPEECH*, 2014.

[28] Adrian Pass, Jianguo Zhang, and Darryl Stewart. An Investigation into Features for Multi-View Lipreading. *ICIP*, 2010.

[29] E.K. Patterson, S. Gurbuz, Z. Tufekci, and J.N. Gowdy. CUAVE: A New Audio-Visual Database for Multimodal Human-Computer Interface Research. *ICASSP*, 2002.

[30] Stavros Petridis and Maja Pantic. Deep Complementary Bottleneck Features for Visual Speech Recognition. *ICASSP*, 2016.

[31] Stavros Petridis, Themos Stafylakis, Pingchuan Ma, Feipeng Cai, Georgios Tzimiropoulos, and Maja Pantic. End-to-End Audiovisual Speech Recognition. *arXiv:1802.06424*, 2018.

[32] Gerasimos Potamianos, Chalapathy Neti, and Giridharan Iyengar. A Cascade Visual Front End for Speaker Independent Automatic Speechreading. *International Journal of Speech Technology*, 2001.

[33] Gerasimos Potamianos, Chalapathy Neti, Guillaume Gravier, Ashutosh Garg, and Andrew W. Senior. Recent Advances in the Automatic Recognition of Audiovisual Speech. *Proceedings of the IEEE*, 2003.

[34] Zhaofan Qiu, Ting Yao, and Tao Mei. Learning Spatio-Temporal Representation with Pseudo-3D Residual Networks. *ICCV*, 2017.

[35] Mike Schuster and Kuldip K Paliwal. Bidirectional Recurrent Neural Networks. *IEEE Transactions on Signal Processing*, 1997.

[36] Xu Shao and Jon Barker. Stream Weight Estimation for Multistream Audio-Visual Speech Recognition in a Multispeaker Environment. *Speech Communication*, 2008.

[37] Karen Simonyan and Andrew Zisserman. Two-Stream Convolutional Networks for Action Recognition in Videos. *NIPS*, 2014.

[38] Karen Simonyan and Andrew Zisserman. Very Deep Convolutional Networks for Large-Scale Image Recognition. *ICLR*, 2015.

[39] Darryl Stewart, Rowan Seymour, Adrian Pass, and Ji Ming. Robust Audio-Visual Speech Recognition under Noisy Audio-Video Conditions. *IEEE Transactions on Cybernetics*, 2014.

[40] Chao Sui, Mohammed Bennamoun, and Roberto Togneri. Listening With Your Eyes: Towards a Practical Visual Speech Recognition System Using Deep Boltzmann Machines. *ICCV*, 2015.

[41] Deqing Sun, Xiaodong Yang, Ming-Yu Liu, and Jan Kautz. PWC-Net: CNNs for Optical Flow Using Pyramid, Warping, and Cost Volume. *CVPR*, 2018.

[42] Christian Szegedy, Wei Liu, Yangqing Jia, Pierre Sermanet, Scott Reed, Dragomir Anguelov, Dumitru Erhan, Vincent Vanhoucke, and Andrew Rabinovich. Going Deeper with Convolutions. *CVPR*, 2015.

[43] Yuki Takashima, Ryo Aihara, Tetsuya Takiguchi, and Yasuo Ariki. Audio-Visual Speech Recognition Using Bimodal-Trained Bottleneck Features for a Person with Severe Hearing Loss. *INTERSPEECH*, 2016.

[44] Graham W Taylor, Rob Fergus, Yann Lecun, and Christoph Bregler. Convolutional Learning of Spatio-Temporal Features. *ECCV*, 2010.

[45] Georgios Tzimiropoulos Themos Stafylakis. Combining Residual Networks with LSTMs for Lipreading. *INTERSPEECH*, 2017.

[46] Du Tran, Lubomir Bourdev, Rob Fergus, Lorenzo Torresani, and Manohar Paluri. Learning Spatiotemporal Features with 3D Convolutional Networks. *ICCV*, 2015.

[47] Michael Wand, Jan Koutník, and Jürgen Schmidhuber. Lipreading with Long Short-Term Memory. *ICASSP*, 2016.

[48] Zuxuan Wu, Yu-gang Jiang, Xi Wang, Hao Ye, and Xiangyang Xue. Multi-Stream Multi-Class Fusion of Deep Networks for Video Classification. *ACMMM*, 2016.

[49] Hong Xiaopeng, Yao Hongxun, Wan Yuqi, and Chen Rong. A PCA Based Visual DCT Feature Extraction Method for Lipreading. *International Conference on Intelligent Information Hiding and Multimedia Signal Processing*, 2006.

[50] Yi Zhu, Zhenzhong Lan, Shawn Newsam, and Alexander G. Hauptmann. Hidden Two-Stream Convolutional Networks for Action Recognition. *ACCV*, 2018.